A BOUNDARY INTEGRAL EQUATION FORMULATION FOR POTENTIAL COMPRESSIBLE FLOWS AROUND DEFORMABLE BODIES

Edoardo Levati[1], Claudio Pasquali[1], Giovanni Bernardini[1] & Massimo Gennaretti[1]

[1]Roma Tre University, Rome, Italy, 00146

Abstract

This paper presents a boundary integral formulation for the aerodynamic analysis of deformable lifting bodies in compressible potential flows. The body contribution is expressed in a body-fitted curvilinear coordinate system (material body description). Instead, the wake contribution, which is the critical element in this kind of problems, is described through two different but equivalent formulations, both applicable also in a free-wake solution mode: (i) a material wake description and (ii) a surface-fitted Lagrangian description. The numerical investigation is aimed at validating the proposed formulations. First, for a simple non-lifting body problem the integral formulation is validated against the analytical solution for the potential field generated by a moving pulsating source. Then, the two alternative formulations for lifting bodies are cross-validated in the case of the flight of a deformable bending wing at several Mach numbers. These results prove the capability of the proposed approaches to solve lifting-body problems and their equivalence.

Keywords: aerodynamics; compressible potential flows; free-wake; lifting deforming bodies

1. Introduction

Current developments in aviation design and the increased demand for innovative aircraft, even with unconventional geometry, require more reliable and high-performance computational tools for aerodynamic and aeroacoustic analyses.

A key aspect of aircraft design concerns the aerodynamic analysis and thus the prediction of air loads generated by lifting surfaces. This becomes a challenging task when the designers deal with highly flexible structures typical of innovative aircraft configurations, for which the aeroelastic phenomena may generate significant deformations of the body that cannot be neglected in solving the aerodynamic field.

The aeroelastic loop must be accounted for a correct and efficient design of aircraft structures [1, 2]. This phenomenon can be examined either experimentally or through a computational analysis [3, 4]. The former presents reliable results but is very expensive, time-consuming, and fitted for a specific aeronautical configuration. Also numerical studies are time-consuming when accomplished through application of CFD high-fidelity solvers. However, in the early stages of aircraft design (i.e., conceptual and preliminary phases), the interest of the designers focuses on formulations capable of producing accurate results with acceptable computational time.

The computational tools based on boundary integral equation formulations for the aerodynamic analysis of bodies moving in potential flows meet the time constraint while maintaining a good level of accuracy [5, 6], and the ability to analyze complex aircraft configurations. In this context, the free-wake analysis of lifting deformable bodies in compressible flows is still an open problem, to the authors' knowledge. The availability of such an aerodynamic solution tool could be of great help not only in the design of highly flexible fixed-wing aircraft but also in the design of rotorcraft. Indeed, in the latter applications the rotor wakes present highly distorted shapes, especially when strong blade-vortex-interaction (BVI) phenomena occur, and the combination of compressibility effects and wake shape deformation must be accurately captured by the computational tools in order to obtain reliable aerodynamic simulations.

This paper presents a novel boundary integral equation formulation suitable for the aerodynamic analysis of flexible bodies moving in compressible potential flows, which can be considered as an extension of those developed in the past for rigid bodies [5, 7, 8]. It considers a surface-fitted curvilinear coordinate system to describe the contributions from the different boundary surfaces. Specifically, the body contribution is expressed through a body-fitted curvilinear coordinate system (material body description), while the wake contribution can be expressed by two alternative but theoretically equivalent formulations: (i) a material wake description in which the curvilinear coordinates follow the wake material points, and (ii) a surface-fitted Lagrangian description in which the wake material points move with respect to the curvilinear coordinate system.

The paper is organized as follows. First, section 2. presents the boundary integral equation formulation for generic deformable surfaces moving in compressible flows. Then, section 3. shows the application of the formulation to deformable lifting bodies. Finally, section 4. presents the numerical investigation aimed at validating the proposed formulations. Specifically, for a non-lifting body problem the formulation is validated against the analytical solution of a moving pulsating velocity potential source, while the two alternative formulations for lifting bodies are numerically cross-validated for the problem of the evaluation of aerodynamic loads arising on deformable bending wings.

2. A Boundary Integral Equation Formulation for Potential Compressible Flows Around Deformable Surfaces

Let us consider a reference system rigidly connected with the undisturbed inviscid fluid, $R(\mathbf{x})$, for which the perturbation flow velocity is described through the velocity potential. Then, the problem governing the propagation of the velocity potential perturbations, $\phi(\mathbf{x},t)$, can be written as [7]

$$\nabla^2\bar{\phi} - \frac{1}{c^2}\frac{\partial^2\bar{\phi}}{\partial t^2} = \sigma H + \nabla\phi\cdot\nabla H + \nabla\cdot(\phi\nabla H) - \frac{1}{c^2}\frac{\partial\phi}{\partial t}\frac{\partial H}{\partial t} - \frac{1}{c^2}\frac{\partial}{\partial t}(\phi\frac{\partial H}{\partial t}) \tag{1}$$

where c indicates the speed of sound in the undisturbed fluid and σ is a nonlinear term which is non-negligible in the transonic regime.

In the above equation $\bar{\phi} = \phi H(f)$ extends ϕ to the whole domain $\mathbb{R}^3$, with $H(f)$ denoting the Heaviside function, and $f(\mathbf{x},t) = 0$ representing the surface bounding the fluid domain where the signal propagation is described by eq. (1).

To derive the solution of eq. (1), the free-space Green's functions method is used [9, 10]. Specifically, following [11, 12] the Lagrangian Green's function is derived as

$$\check{G}(\mathbf{x},\mathbf{x}_*,t,t_*) = \left.\frac{-1}{4\pi r(1+M_r)}\right|_{\check{g}=0}\delta(t-t_*+\check{\theta}) = \check{G}_0\delta(t-t_*+\check{\theta}) \tag{2}$$

where $r = |\mathbf{x}-\mathbf{x}_*|$, with $\mathbf{x}$ and $\mathbf{x}_*$ denoting, respectively, source and the observer points, t indicates the emission time and t_* is the observer time. In addition, $\mathbf{M}$ represents the Mach number related to the velocity of the source point, and M_r denotes its projection onto the direction observer-source distance vector. Furthermore, $\check{\theta}$ denotes the time taken by the signal to propagate between these two points, whereas, the symbol $|_{\check{g}=0}$ represents the evaluation at the signal emission time, $t = t_* - \check{\theta}$.

Then, by introducing a surface-fitted curvilinear coordinate system (ξ_1,ξ_2,ξ_3) such that $\xi_3(\mathbf{x},t) = 0$ identifies the boundary surface points, it is possible to map them onto the plane $(\xi_1,\xi_2,0)$) through the function $\mathbf{x} = \mathbf{X}(\xi_i,t)$.

Thus, following a procedure similar to that presented in [8, 9, 12, 13, 14], the boundary integral equation formulation solution of eq. (1) for deformable boundary surfaces in arbitrary motion in compressible flows is given by the expression

$$\bar{\phi}(\xi_*,t_*) = \int_\Omega \left[\check{G}_0\frac{\partial\phi}{\partial\check{n}} + \dot{\phi}\check{G}_0\left(\frac{\partial\check{\theta}}{\partial\check{n}} + 2\frac{M_n}{c}\right) + \phi\left(-\frac{\partial\check{G}_0}{\partial\check{n}} + \check{G}_0\left.\frac{\partial D}{\partial t}\right|_\xi\right)\right]J\bigg|_{\check{g}=0} d\xi_1 d\xi_2 \tag{3}$$

where M_n is the projection of the Mach number onto the direction normal to the surface, $J(\xi_1,\xi_2,t)$ is the Jacobian of the transformation $\mathbf{x} = \mathbf{X}(\xi_i,t)$ and $\check{\mathbf{n}} = \mathbf{n} - M_n\mathbf{M}$. In addition,

$$\left.\frac{\partial D}{\partial t}\right|_\xi = \frac{1}{J}\left.\frac{\partial}{\partial t}\right|_\xi\left[J\left(\frac{\partial\check{\theta}}{\partial\check{n}} + \frac{M_n}{c}\right)\right] \tag{4}$$

Note that when eq. (3) is used as an integral equation, it presents a singular doublet contribution which produces a free term equal to 1/2 (see [15] for details). The remaining contribution is, thus, evaluated as the principal Cauchy value.

3. Aerodynamics Boundary Integral Equation Formulation for Deformable Lifting Bodies

As shown in [5, 8, 10], in the case of the perturbation field generated by lifting bodies the potential solution is given by the superposition of body and wake contributions.
While the most convenient and natural way to evaluate the body contribution is to use a body-fitted curvilinear coordinates system following the body surface material points, the wake contribution can be described in two different, but theoretically equivalent, forms: (i) a material wake description in which the curvilinear coordinates follow the wake material points, and (ii) a surface-fitted Lagrangian description in which the wake material points move with respect to the curvilinear coordinate system. The corresponding two different boundary integral equation formulations are presented in the following two subsections.

3.1 Material Wake Description

To derive the integral equation with the surface material wake description (MW), each point of the wake surface is identified by the curvilinear coordinate system (λ, α), where λ represents the span position of the trailing edge point from which the wake point was released, while α denotes the time of release (i.e., $\alpha = 0$ corresponds to the initial time and α_* denotes the current time). Thus, a line $\alpha =$constant identifies the locus of the material wake points that were at the trailing edge at a given time, $t = \alpha$, while a line $\lambda =$constant identifies all points emitted from the the same trailing edge point. In this framework, the wake surface progressively grows while the trailing edge moves.
In compressible flows, due to signal propagation delay, not all wake points affect the potential solution at a given observer point at a given time [11]. Thus, for a given observer point and a given observation time, effective and non-effective sub-domains of the wake surface can be identified, separated by a line defined by the coordinate $\breve{\alpha} = \alpha(\alpha_*, \lambda, \xi_*)$. From these observations, the following boundary integral formulation for the velocity potential generated by lifting wings is derived

$$\bar{\phi}(\xi_*, t_*) = \int_{S_b} \left[\breve{G}_0 \frac{\partial \phi}{\partial \breve{n}} + \dot{\phi} \breve{G}_0 \left(\frac{\partial \breve{\theta}}{\partial \breve{n}} + 2\frac{M_n}{c} \right) + \phi \left(-\frac{\partial \breve{G}_0}{\partial \breve{n}} + \breve{G}_0 \frac{\partial D}{\partial t} \right) \right] J \bigg|_{\breve{g}=0} d\xi_1 d\xi_2 \; + $$

$$+ \int_{S_{\hat{w}}} \left[\Delta\phi \left(-\frac{\partial \breve{G}_0}{\partial \breve{n}} + \breve{G}_0 \frac{\partial D}{\partial t} \right) - \breve{G}_0 M_n \mathbf{M} \cdot \Delta \mathbf{V}_t \right] J_w \bigg|_{\breve{g}=0} d\alpha d\lambda + \int_{\lambda_1}^{\lambda_2} \left[\Delta\phi G_0 \frac{\partial \theta}{\partial n} \frac{J_w}{h_w} \right] \bigg|_{\alpha=\breve{\alpha}} d\lambda \qquad (5)$$

where the first integral is the body contribution, the second is the effective wake surface contribution and the third is an integral over the separation line between the effective and the non-effective wake portions. Note that, in case of free-wake mode analysis in which the shape of the wake is determined as part of the solution by moving the the wake points accordingly to the velocity field self-induced by the wake vorticity, the Mach number in eq. (5) corresponds to the local induced velocity.

In eq. (5), $\Delta \mathbf{V}_t = \Delta \nabla_t \phi$ is the difference between the tangential fluid velocity evaluated over the upper and lower wake surfaces, $(\mathbf{a}_\lambda, \mathbf{a}_\alpha)$ are the covariant base vectors, $J_w = |\mathbf{a}_\lambda \times \mathbf{a}_\alpha|$ is the Jacobian of the transformation, and $[\lambda_1, \lambda_2]$ represent the root and tip points of the trailing edge. Furthermore, the Kutta-Morino condition [10] allows us to obtain $\Delta\phi$ from the time history of the jump of the velocity potential calculated at the trailing edge. Finally, note that, the deformation velocity of the separation line is zero (at the time of release from the trailing edge they are fixed with the undisturbed air), and thus in the line integral we have $G_0 = -1/4\pi r$, $\theta = r/c$, and $h_w = |1 + \mathbf{a}_\alpha \cdot \nabla\theta|$.

3.2 Surface-Fitted Lagrangian Wake Description

Since the numerical evaluation of the line-integral contribution in eq. (5) is quite critical and implies a low rate of convergence, it is useful to consider an alternative formulation that does not present a

line contribution. This can be obtained by using a surface-fitted Lagrangian wake description where the curvilinear coordinate system (α,λ) is such that, as in the previous case, λ, represents the radial position of the trailing edge point from which the wake material point was released, while α originates from the current position of the trailing edge and can be identified with a backward time shift (i.e., $\alpha = 0$ denotes the trailing edge $\forall t$) [8, 16]. Note that, following this approach, for instance, once the steady-state condition is reached for a free-wake analysis of a translating wing, each (α,λ) wake geometric point moves with the same trailing edge body velocity.
Thus, it can be shown that the following boundary integral formulation for the potential function is derived through the surface-fitted Lagrangian wake description (SFW)

$$\bar{\phi}(\xi_*,t_*) = \int_{S_b} \left[\check{G}_0 \frac{\partial \phi}{\partial \check{n}} + \dot{\phi}\check{G}_0 \left(\frac{\partial \check{\theta}}{\partial \check{n}} + 2\frac{M_n}{c} \right) + \phi \left(-\frac{\partial \check{G}_0}{\partial \check{n}} + \check{G}_0 \frac{\partial D}{\partial t} \right) \right] J \Big|_{\check{g}=0} d\xi_1 d\xi_2 \quad +$$

$$\int_{S_w} \left[-\check{G}_0 M_n \mathbf{M}\cdot\Delta\mathbf{V}_t + \Delta\dot{\phi}\check{G}_0 \left(\frac{\partial \check{\theta}}{\partial \check{n}} + 2\frac{M_n}{c} \right) + \Delta\phi \left(-\frac{\partial \check{G}_0}{\partial \check{n}} + \check{G}_0 \frac{\partial D}{\partial t} \right) \right] J_w \Big|_{\check{g}=0} d\alpha d\lambda \qquad (6)$$

where the first integral is the contribution of the body and the second integral is the contribution of the wake surface. In this formulation, no line-integral contribution appears.
Note that, in eq. (6) the Mach number in the wake contribution corresponds to the velocity of the wake geometric points identified by the (α,λ) coordinates.

4. Numerical Results

This section presents the numerical results obtained with the new formulation. In section 4.1, the validation of the formulation for the non-lifting bodies (Eq. (3)) is validated against the analytical solution of a pulsating source, while section 4.2 shows a cross-correlation of the formulations for lifting bodies (Eqs. (5) and (6)) applied to a deforming wing with a fixed wake.

4.1 Pulsating Moving Source Surrounded by a Porous Surface

This analysis consists of the comparison between the potential field generated by a pulsating velocity potential source evaluated analytically and that given by the proposed boundary integral formulation applied to a deforming porous surface wing that surrounds the source, considering the analytical normal derivative of the potential over the body as input [17, 18].
The wing has a span equal to 3m, the chord length is equal to 1m, and the sections have a lenticular shape with the maximum thickness equal to the 40% of the chord length. The numerical analysis is accomplished for different Mach numbers and body deforming through the combination of harmonic bending and torsion deflections.
The results are shown in figs. 1a to 1c in term of the potential evaluated at three different body points for the source pulsating at frequency $\omega_s = 3Hz$ and bending and torsion frequencies equal to, respectively, $\omega_b = 1Hz$ and $\omega_t = 2Hz$. These figures show a perfect agreement between the analytical and the numerical solution, thus proving the capability of the proposed formulation to capture perturbation fields in deforming-boundary domains.

4.2 Deforming Lifting Wing with Fixed Wake

The cross-validation of the two aerodynamic formulations for lifting bodies presented in sections 3.1 and 3.2 is performed by considering a lifting deforming wing with span $b = 10$ m, chord length $c = 1$ m, and angle of attack equal to $\alpha = 5°$. The wing is assumed to be subject to bending deformations and three flight Mach numbers are considered ($M = 0.5, 0.6, 0.7$). Two harmonic bending deformations with frequency $\omega_b = 1$ Hz are considered. The ratio between their amplitudes is $A_2/A_1 = 3.25$.
Note that although the formulations presented in sections 3.1and 3.2 allow for a free wake analysis, all the results are obtained by assuming a fixed wake model, thus neglecting the wake deformation due to the induced velocity (i.e., the wake surface coincides with the locus of the points swept by the trailing edge).
Examples of the wake geometry considered in the two proposed wake formulations are given in fig. 2 and fig. 3. Specifically, fig. 2 shows the wake as deriving from the material description MW. It

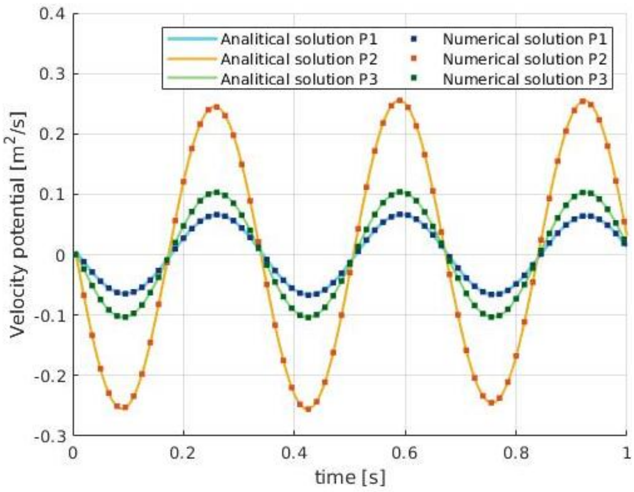

(a) $M = 0.4$.

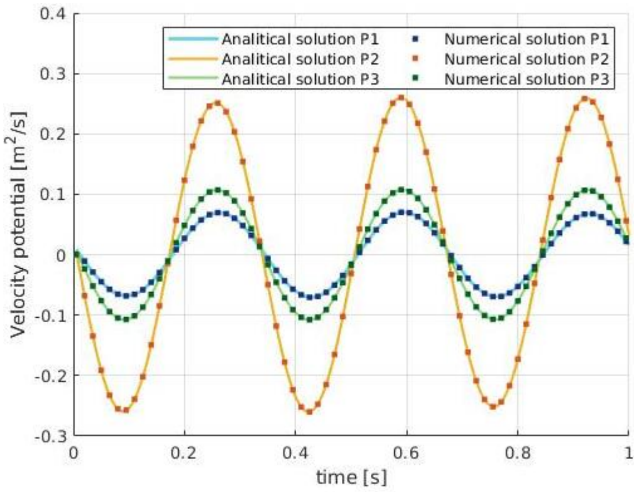

(b) $M = 0.5$.

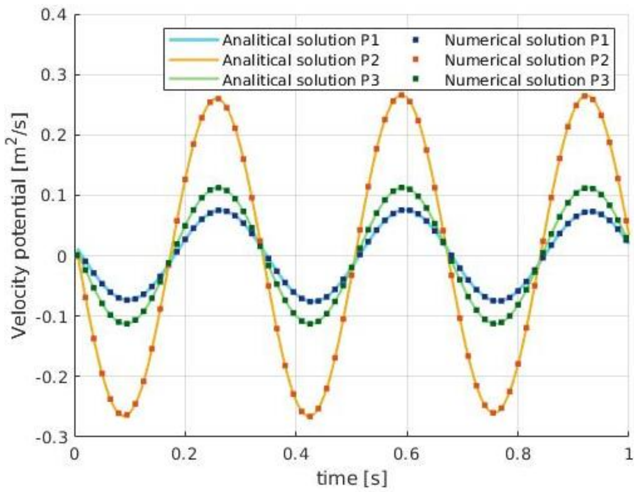

(c) $M = 0.6$.

Figure 1 – Comparison between the velocity potential time history on three different body control points evaluated analytically and numerically.

is interesting to note that by varying the observer point compressibility effects alter the geometrical locus of the separation line between the influencing and non-influencing wake. Instead fig. 3 shows the wake corresponding to the non-material wake description, SFW.
Then, for both bending configurations and three Mach numbers, figs. 4a and 4b present the solutions from the two formulations evaluated in terms of the converged time history of the lift coefficient (C_L) (the convergence is accomplished in terms of the number of discretization panels used over the wing and the wake). The agreement between the predictions of the two formulations is excellent, thus proving their full equivalence.
This conclusion is confirmed by the results in table 1, which shows, for both configurations analyzed, the relative squared error (RSE) of the time history of C_L predicted by the two formulations. Indeed, the maximum deviation is 0.53% in the worst case.

Table 1 – Relative squared error of the lift coefficient varying Mach number.

M	0.5	0.6	0.7
Conf-1	0.45%	0.25%	0.51%
Conf-2	0.08%	0.20%	0.53%

Finally, considering the flight condition at $M = 0.7$ and configuration-2, figs. 5a to 5d show the comparison between the chordwise pressure coefficient, C_P, at the section located at 80% of the span for

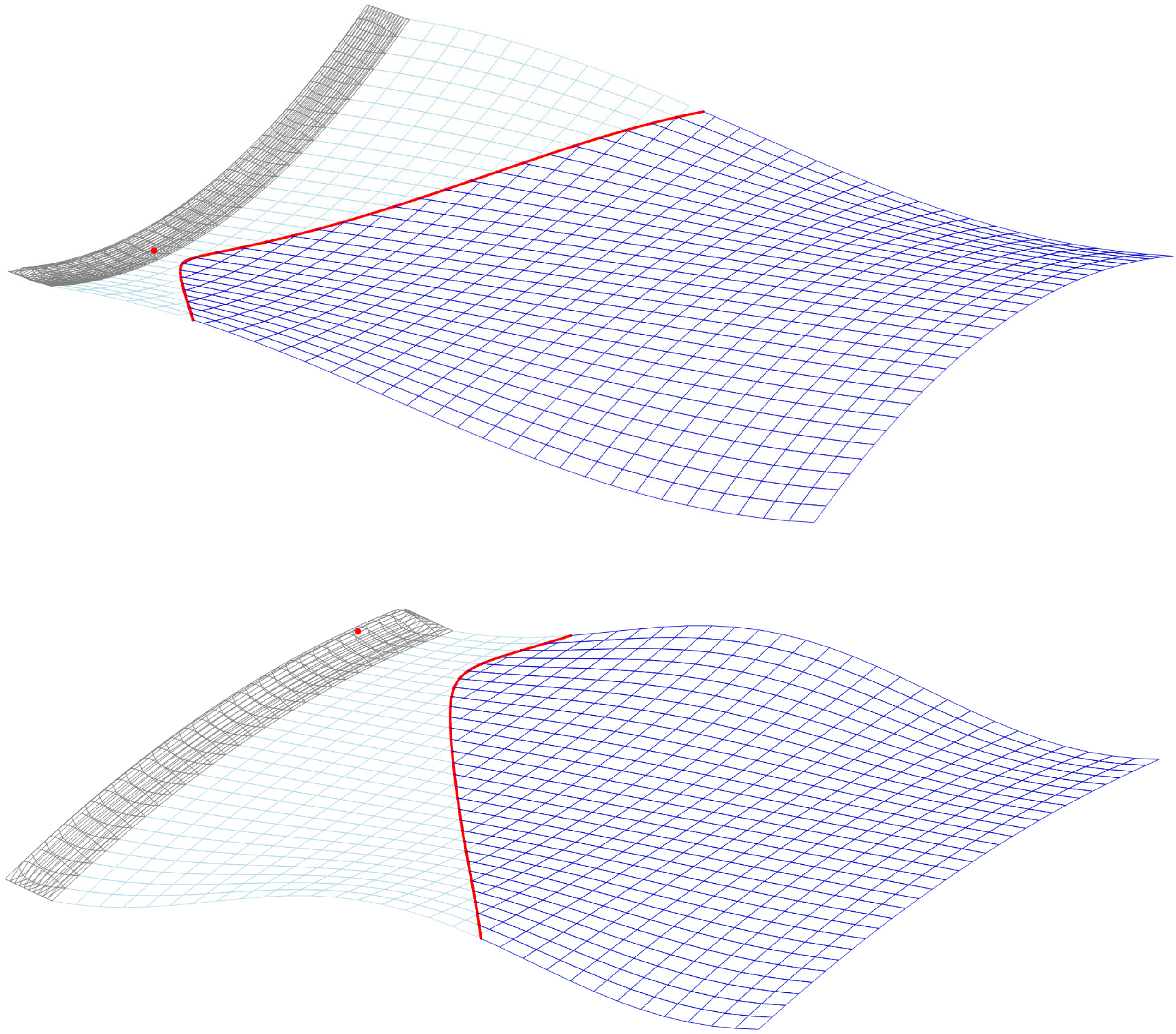

Figure 2 – Sketches of the MW description. Grey surface: deformed wing; red bullet: observer point; red line: separation line between influencing and non-influencing wake portions; dark blue surface: influencing wake portion; light blue surface: non-influencing wake portion.

four-time instants evaluated by the two wake formulations. Again, the agreement is perfect. Note that although not shown here, this level of agreement is maintained for other spanwise sections and all Mach numbers and configurations examined.

5. Conclusions

This paper has presented a boundary integral formulation for the aerodynamic analysis of deformable lifting bodies moving in compressible potential flows. It is capable of performing free-wake analyses where the shape of the wake is determined as part of the solution. The body surface contribution is described through the introduction of a surface-fitted material curvilinear coordinate system. Instead, the wake contribution, which can be considered as the critical element in this kind of aerodynamic formulation, is expressed by two different but equivalent formulations: one derived from the application of a material curvilinear coordinate system for the mapping of the wake surface, and a second one which still considers a surface-fitted curvilinear coordinate system for the surface mapping which, however, defines geometric and not material wake points. By considering a pulsating source surrounded by a porous deforming surface, the results of the numerical investigation have first validated the capability of the proposed formulation to describe perturbation fields of the velocity potential in

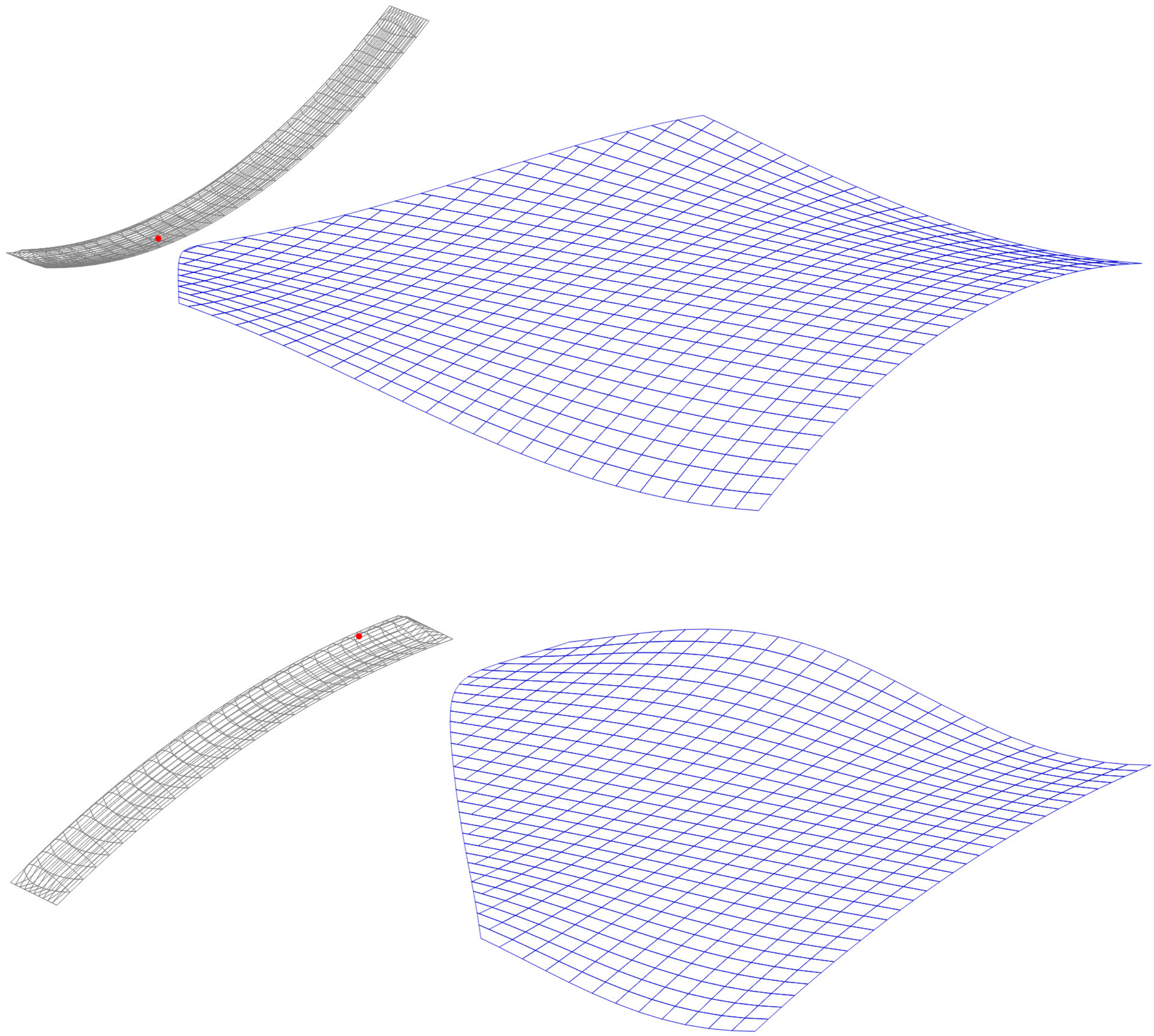

Figure 3 – Sketches of the SFW description. Grey surface: deformed wing; red bullet: observer point; dark blue surface: wake surface.

fluid domains bounded by deforming surfaces. Then, a bending lifting wing has been examined by applying the two formulations for the wake description, and the outcomes of the investigation have confirmed their perfect equivalence. Thus, the results of this paper can be considered as a first step towards the validation of the proposed deformable-boundary integral formulation for the free-wake aerodynamic analysis of lifting bodies in arbitrary motion in compressible flows. To the authors' knowledge, this kind of approach is novel in the field of boundary element methods. It can be of great interest to aircraft designers since it represents a good trade-off between simulation accuracy and computational cost. Finally, it is worth mentioning that this type of formulation can be extremely efficient for rotorcraft aerodynamic analyses where the wake shape plays a fundamental role, especially in problems dominated by strong blade-vortex interaction phenomena.

6. Contact Author Email Address

edoardo.levati@uniroma3.it

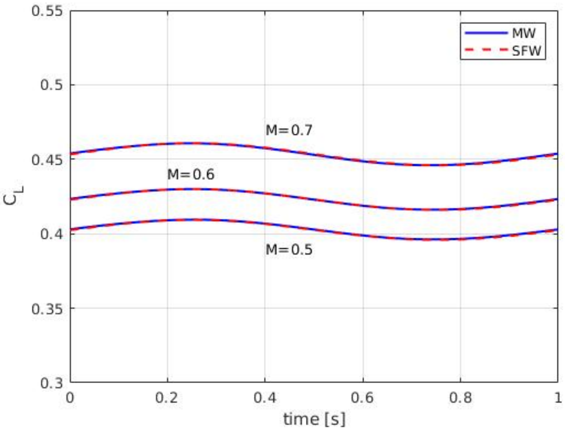

(a) Configuration-1.

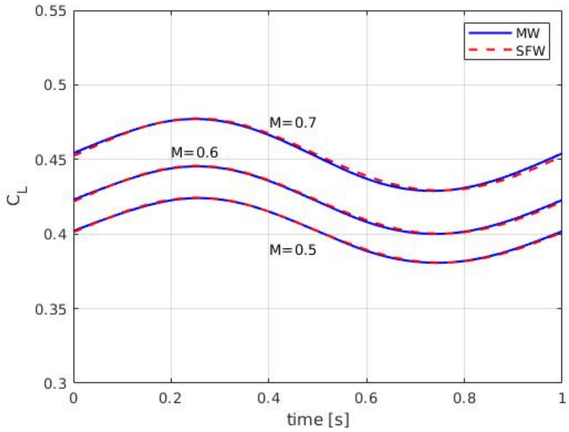

(b) Configuration-2.

Figure 4 – Lift coefficient time history at three different Mach numbers.

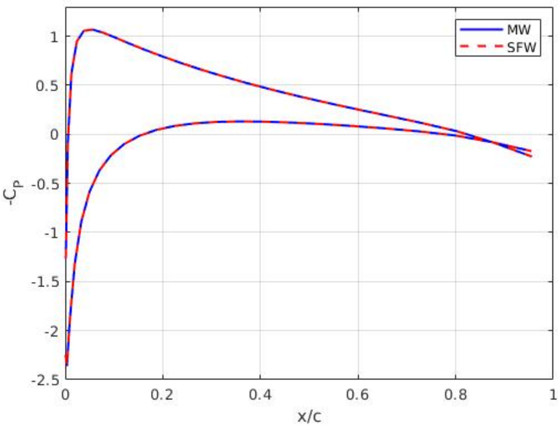

(a) $t = 0.25s$

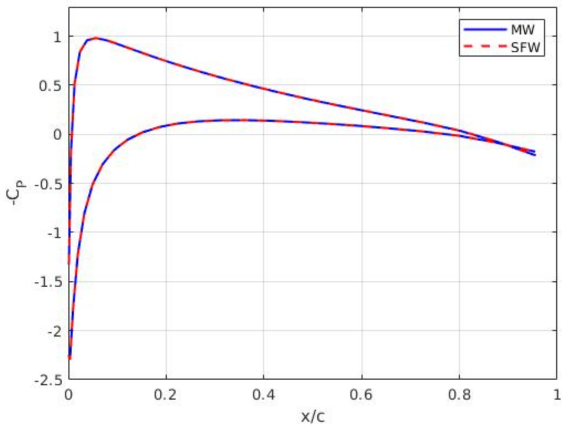

(b) $t = 0.50s$

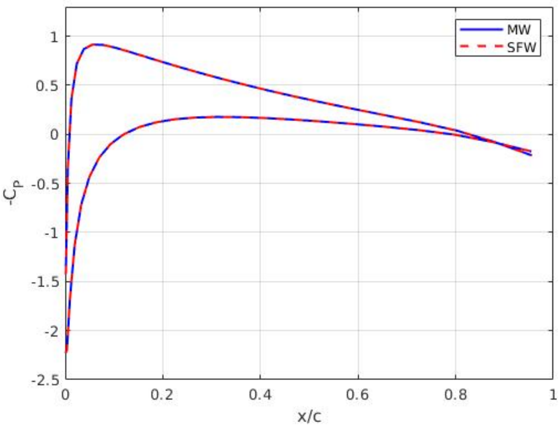

(c) $t = 0.75s$

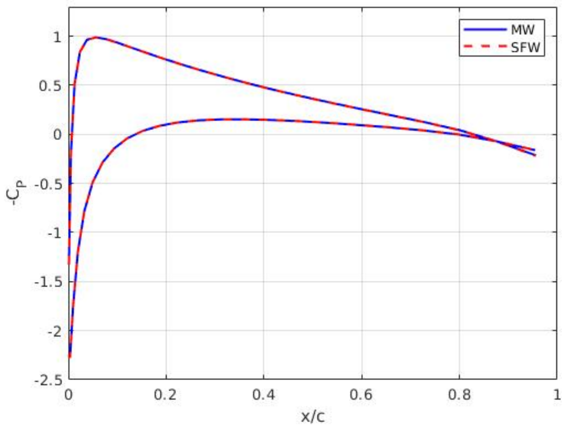

(d) $t = 1s$

Figure 5 – Pressure coefficient at section $y/b = 0.8$, configuration-2, $M = 0.7$.

7. Copyright Statement

References

[1] Gennaretti M and Bernardini G. Aeroelastic response of helicopter rotors using a 3d unsteady aerodynamic solver. *The Aeronautical Journal*, Vol. 110, No. 1114, pp 793–801, 2006.

[2] Kamakoti R and Shyy W. Fluid–structure interaction for aeroelastic applications. *Progress in Aerospace Sciences*, Vol. 40, No. 8, pp 535–558, 2004.

[3] Prapamonthon P, Yin B, Yangi G and Lu M, Zhang P. Recent progress in flexibility effects on wing aerodynamics and acoustics. *Proceedings of the Institution of Mechanical Engineers, Part C: Journal of Mechanical Engineering Science*, Vol. 235, No. 2, pp 208–244, 2021.

[4] Shyy W, Aono H, Chimakurthi S-K, Trizila P, Kang C-K, Cesnik C ES and Liu H. Recent progress in flapping wing aerodynamics and aeroelasticity. *Progress in Aerospace Sciences*, Vol. 46, No. 7, pp 284–327, 2010.

[5] Gennaretti M and Bernardini G. Novel boundary integral formulation for blade-vortex interaction aerodynamics of helicopter rotors. *AIAA Journal*, Vol. 45, No. 6, pp 1169–1176, 2007.

[6] Pasquali C, Serafini J, Bernardini G, Milluzzo J and Gennaretti M. Numerical-experimental correlation of hovering rotor aerodynamics in ground effect. *Aerospace Science and Technology*, Vol. 106, pp 106079, 2020.

[7] Morino L, Bharadvaj BK, Freedman MI and Tseng K. Boundary integral equation for wave equation with moving boundary and applications to compressible potential aerodynamics of airplanes and helicopters. *Computational Mechanics*, Vol. 4, No. 4, pp 231–243, 1989.

[8] Gennaretti M. Una formulazione integrale di contorno per la trattazione di flussi aeronautici viscosi e potenziali. Doctoral dissertation, University of Rome 'La Sapienza', 1993.

[9] Morino L and Gennaretti M. A boundary element method for the potential, compressible aerodynamics of bodies in arbitrary motion, *The Aeronautical Journal*, Vol. 96, No. 951, pp 15-19, 1992.

[10] Morino L. *A General Theory of Unsteady Compressible Potential Aerodynamics*. NASA CR- 2464, 1974.

[11] Gennaretti M, Luceri L and Morino L. A unified boundary integral methodology for aerodynamics and aeroacoustics of rotors. *Journal of Sound and Vibration*, Vol. 200, No. 4, pp 467–489, 1997.

[12] Testa C, Poggi C, Bernardini G and Gennaretti M. Pressure-field permeable-surface integral formulations for sound scattered by moving bodies. *Journal of Sound and Vibration*, Vol. 459, pp 14860, 2019.

[13] Gennaretti M, De Rubeis B, Poggi C and Bernardini G. Acoustic analysis of a rotor in forward flight with deformable blades through a boundary integral formulation. *Proc AIAA AVIATION 2023 Forum*, pp 3216, 2023.

[14] De Rubeis B, Gennaretti M, Poggi C and Bernardini G. Boundary integral formulation for sound scattered by deformable bodies. *Proc 30th AIAA/CEAS Aeroacoustics Conference*, pp 3013, 2024.

[15] Gennaretti M and Testa C. A boundary integral formulation for sound scattered by elastic moving bodies. *Journal of Sound and Vibration*, Vol. 314, No. 3-5, pp 712–737, 2008.

[16] Morino L, Bernardini G and Gennaretti M. A boundary element method for the aerodynamic analysis of aircraft in arbitrary motions. *Computational Mechanics*, Vol. 32, pp 301-311, 2003.

[17] Levati E. Una formulazione integrale per flussi potenziali comprimibili attorno a corpi deformabili. Master's thesis in Aeronautical Engineering, Roma Tre University, 2023.

[18] De Rubeis B. Prediction of aeroacoustics of deformable bodies with solid or porous surface through a boundary integral formulation. *Proc Aerospace Science and Engineering: III Aerospace PhD-Days*, Vol. 33, pp 21, 2023.